Testing the Electroweak Theory in Mutliboson Measurements in ATLAS

(ATLAS public results from 2023)

Gia Khoriauli

University of Würzburg

On behalf of ATLAS Collaboration

Lake Louise Winter Institute

Lake Louise, Canada, 18-24 February 2024

Bundesministerium für Bildung und Forschung

Electroweak Multiboson Interactions

- The Standard Model (SM) of elementary particles predicts triple and quartic gauge couplings between the electroweak bosons due to the non-Abelian structure of the electroweak interaction
  - Experimental studies of multiboson interactions are therefore important tests of the SM electroweak theory
  - Effective Field Theory (EFT) frameworks are typically used in model independent searches for new physics effects

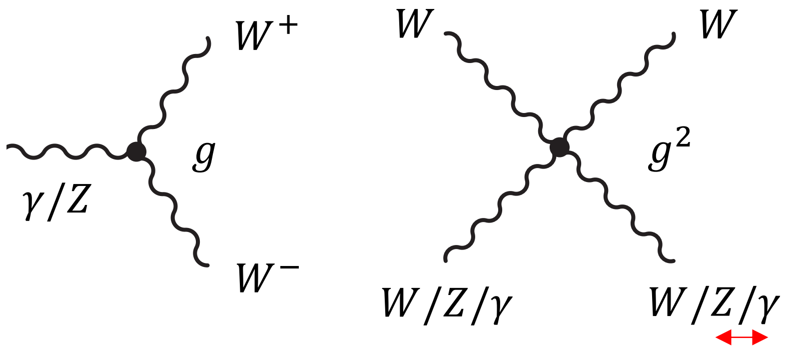

- According to the SM, the massive electroweak bosons obtain their masses and hence, can have longitudinal polarisations via the Higgs mechanism of the spontaneously broken electroweak symmetry
  - Measurements of polarisation observables in the multiboson interactions are the direct probes of this mechanism

- The latest measurements and first observations of the production of different multiboson final states in the ATLAS detector are presented

Same Sign $W^{\pm}W^{\pm}jj$ Measurement

arXiv:2312.00420

$\sqrt{s} = 13\ TeV,\ 139\ fb^{-1}$

- $W^{\pm}W^{\pm}jj$ has the largest ratio of the electroweak to QCD production cross sections among all vector boson scattering (VBS) sensitive $VVjj$ final states
  - As the QCD leading order diagrams with initial gluons are forbidden

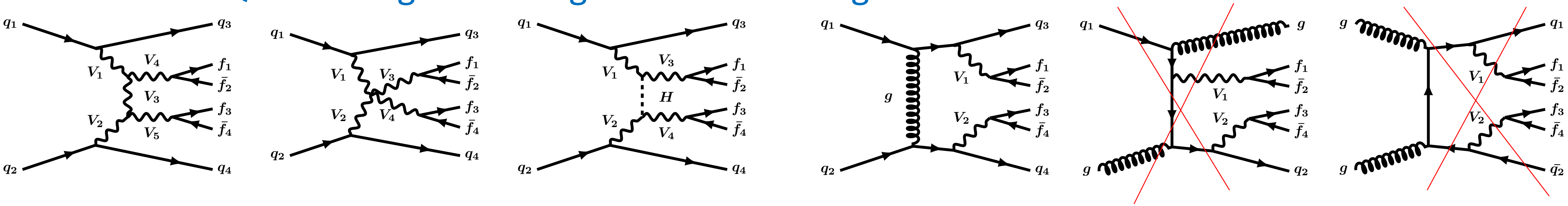

- Fiducial and differential cross sections as functions of different observables are measured for both electroweak and inclusive (EW+QCD) $W^{\pm}W^{\pm}jj$ production

- Good agreement is found for the fiducial cross sections with the SM predictions

Description	$\sigma_{\text{fid}}^{\text{EW}}$ [fb]	$\sigma_{\text{fid}}^{\text{EW+Int+QCD}}$ [fb]
Measured cross section	$2.92 \pm 0.22\,(\text{stat.}) \pm 0.19\,(\text{syst.})$	$3.38 \pm 0.22\,(\text{stat.}) \pm 0.19\,(\text{syst.})$
MG5_AMC+HERWIG7	$2.53 \pm 0.04\,(\text{PDF})\ ^{+0.22}_{-0.19}\,(\text{scale})$	$2.92 \pm 0.05\,(\text{PDF})\ ^{+0.34}_{-0.27}\,(\text{scale})$
MG5_AMC+PYTHIA8	$2.53 \pm 0.04\,(\text{PDF})\ ^{+0.22}_{-0.19}\,(\text{scale})$	$2.90 \pm 0.05\,(\text{PDF})\ ^{+0.33}_{-0.26}\,(\text{scale})$
SHERPA	$2.48 \pm 0.04\,(\text{PDF})\ ^{+0.40}_{-0.27}\,(\text{scale})$	$2.92 \pm 0.03\,(\text{PDF})\ ^{+0.60}_{-0.40}\,(\text{scale})$
SHERPA ⊗ NLO EW	$2.10 \pm 0.03\,(\text{PDF})\ ^{+0.34}_{-0.23}\,(\text{scale})$	$2.54 \pm 0.03\,(\text{PDF})\ ^{+0.50}_{-0.33}\,(\text{scale})$
POWHEG BOX+PYTHIA	2.64	–

Post-fit SR distribution of event yields from differential cross section extraction as a function of m_{ll}

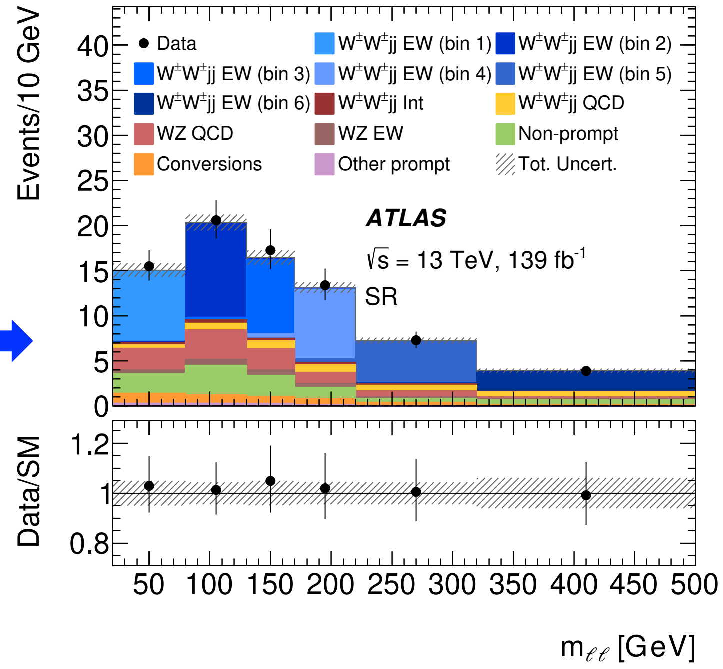

Same Sign $W^{\pm}W^{\pm}jj$ Measurement

- Competitive limits (@ 95% C.L.) are set on the Wilson coefficients of the relevant EFT dimension-8 operators that have large effects on the $WWWW$ coupling
  - The reconstructed m_{ll} distribution is used in the EFT measurements

$$\mathcal{L}_{\text{eff}} = \mathcal{L}_{\text{SM}} + \sum_i \frac{f_i^{(6)}}{\Lambda^2} O_i^{(6)} + \sum_j \frac{f_j^{(8)}}{\Lambda^4} O_j^{(8)}$$

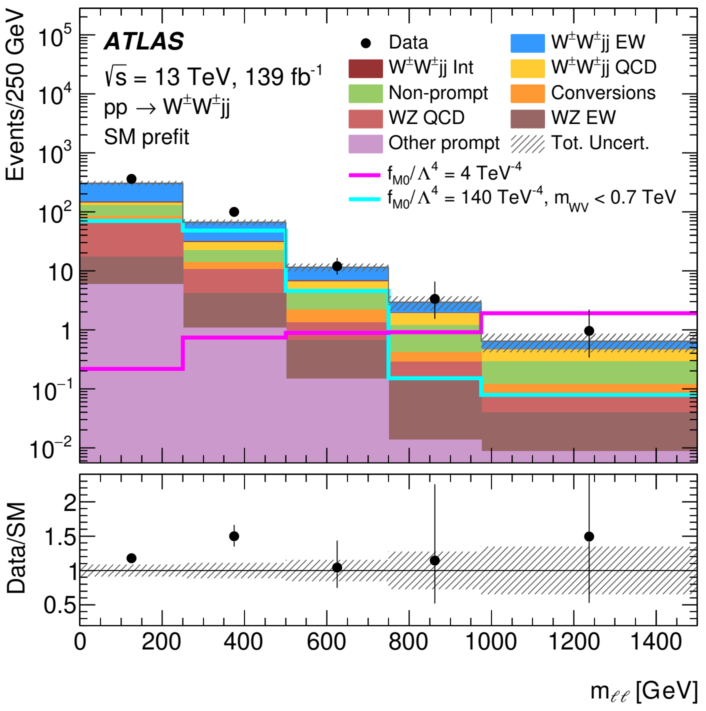

Coefficient	Type	No unitarisation cut-off [TeV^{-4}]	Lower, upper limit at the respective unitarity bound [TeV^{-4}]
f_{M0}/Λ^4	Exp.	[-3.9, 3.8]	-64 at 0.9 TeV, 40 at 1.0 TeV
	Obs.	[-4.1, 4.1]	-140 at 0.7 TeV, 117 at 0.8 TeV
f_{M1}/Λ^4	Exp.	[-6.3, 6.6]	-25.5 at 1.6 TeV, 31 at 1.5 TeV
	Obs.	[-6.8, 7.0]	-45 at 1.4 TeV, 54 at 1.3 TeV
f_{M7}/Λ^4	Exp.	[-9.3, 8.8]	-33 at 1.8 TeV, 29.1 at 1.8 TeV
	Obs.	[-9.8, 9.5]	-39 at 1.7 TeV, 42 at 1.7 TeV
f_{S02}/Λ^4	Exp.	[-5.5, 5.7]	-94 at 0.8 TeV, 122 at 0.7 TeV
	Obs.	[-5.9, 5.9]	–
f_{S1}/Λ^4	Exp.	[-22.0, 22.5]	–
	Obs.	[-23.5, 23.6]	–
f_{T0}/Λ^4	Exp.	[-0.34, 0.34]	-3.2 at 1.2 TeV, 4.9 at 1.1 TeV
	Obs.	[-0.36, 0.36]	-7.4 at 1.0 TeV, 12.4 at 0.9 TeV
f_{T1}/Λ^4	Exp.	[-0.158, 0.174]	-0.32 at 2.6 TeV, 0.44 at 2.4 TeV
	Obs.	[-0.174, 0.186]	-0.38 at 2.5 TeV, 0.49 at 2.4 TeV
f_{T2}/Λ^4	Exp.	[-0.56, 0.70]	-2.60 at 1.7 TeV, 10.3 at 1.2 TeV
	Obs.	[-0.63, 0.74]	–

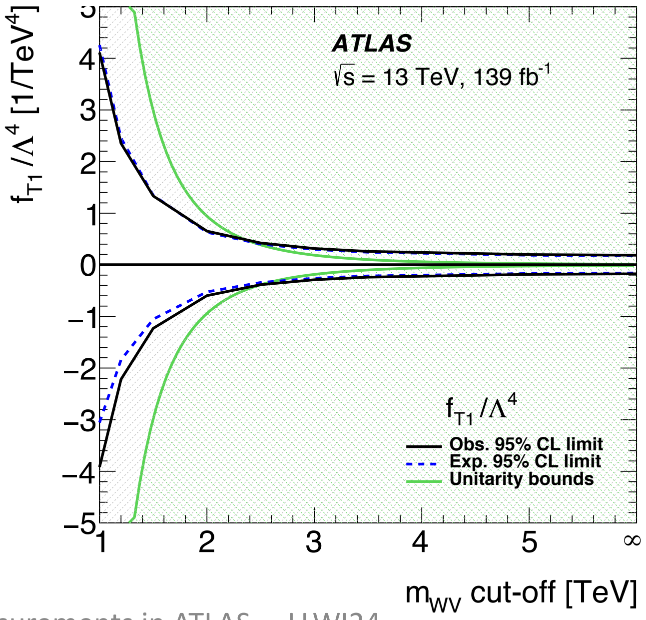

Observation of Opposite Sign W^+W^-jj

ATLAS-CONF-2023-039

$\sqrt{s} = 13\,TeV,\ 140\,fb^{-1}$

- ATLAS observed the electroweak VBS W^+W^-jj production in fully leptonic final states
  - Leptons are required to have different flavours

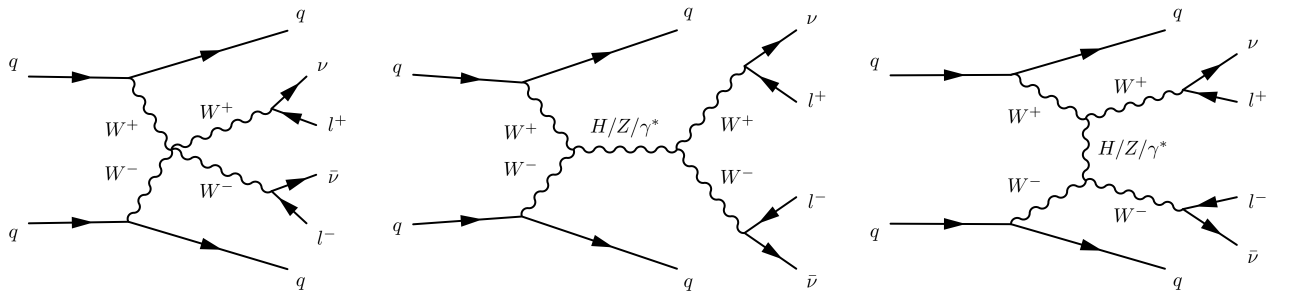

- Top quark (mainly the $t\bar{t}$) along with QCD W^+W^-jj production make huge background to the signal
  - 66% and 24% contributions to the total (post-fit) event prediction in the inclusive signal region, respectively

Process	Event yields $n_{\text{jets}} = 2$	Event yields $n_{\text{jets}} = 3$
EWK W^+W^-jj	158 ± 27	54 ± 13
Top quark	2885 ± 214	1851 ± 131
Strong W^+W^-jj	1214 ± 256	514 ± 121
W+jets	37 ± 97	19 ± 48
Z+jets	216 ± 62	65 ± 25
Multiboson	101 ± 5	42 ± 3
SM prediction	4610 ± 77	2546 ± 48
Data	4610	2533

- Signal region is split into the exclusive 2- and 3-jet event categories to enhance the sensitivity

- Control region for the top quark background is defined by requiring one of the two leading jets to be b-tagged

Observation of Opposite Sign W^+W^-jj

- ❑ Neural Network based discriminant is used to distinguish the signal from background
  - ❖ Signal, top quark and QCD background events are used in the NN training
- ❑ Profile-likelihood fit method is used to fit simultaneously the signal, top and QCD background normalisations in the NN output in the 1 control and 2 signal regions
- ❑ Observed (expected) signal significance is **7.1σ (6.2σ)**
  - ❖ Statistical uncertainty of the measured signal normalisation is **12.3%** with **18.5%** total uncertainty

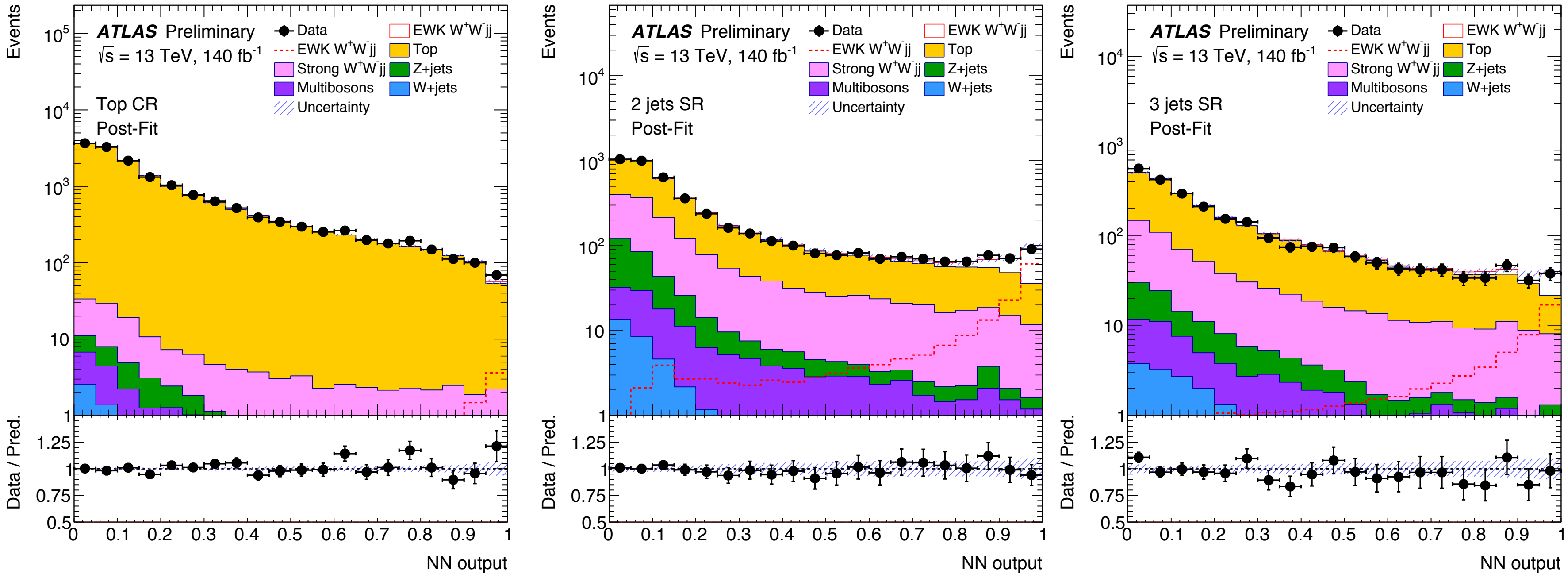

- ❑ Signal fiducial cross section is measured to $\mathbf{2.65^{+0.52}_{-0.48}}\ \boldsymbol{fb}$ vs. predicted $\mathbf{2.20^{+0.14}_{-0.13}}\ \boldsymbol{fb}$
  - ❖ Fiducial volume defined closely to detector level selection but requiring $m_{jj} > 500\ GeV$

Opposite Sign W^+W^- Cross-Sections

ATLAS-CONF-2023-012

$\sqrt{s} = 13\ TeV,\ 140\ fb^{-1}$

- Fiducial and differential cross sections are measured in $W^+W^- \rightarrow e^{\pm}\nu\mu^{\mp}\nu$ final states
  - The fiducial cross section is extrapolated to the full phase-space of W^+W^- production
- Top-quark background is precisely estimated in bins of the signal region with the help of two dedicated control regions
  - Defined by requiring exactly 1 and exactly 2 b-jets, respectively
  - No constraints on the jet multiplicity
- Fiducial cross section is measured using profile-likelihood fit with the free signal normalisation to the detector-level S_T distribution
  - S_T - scalar sum of all jet and lepton transverse momenta

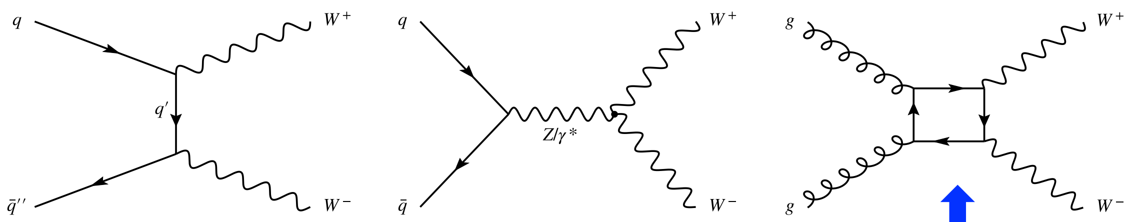

Provides ~5% contibution in the WW production rate

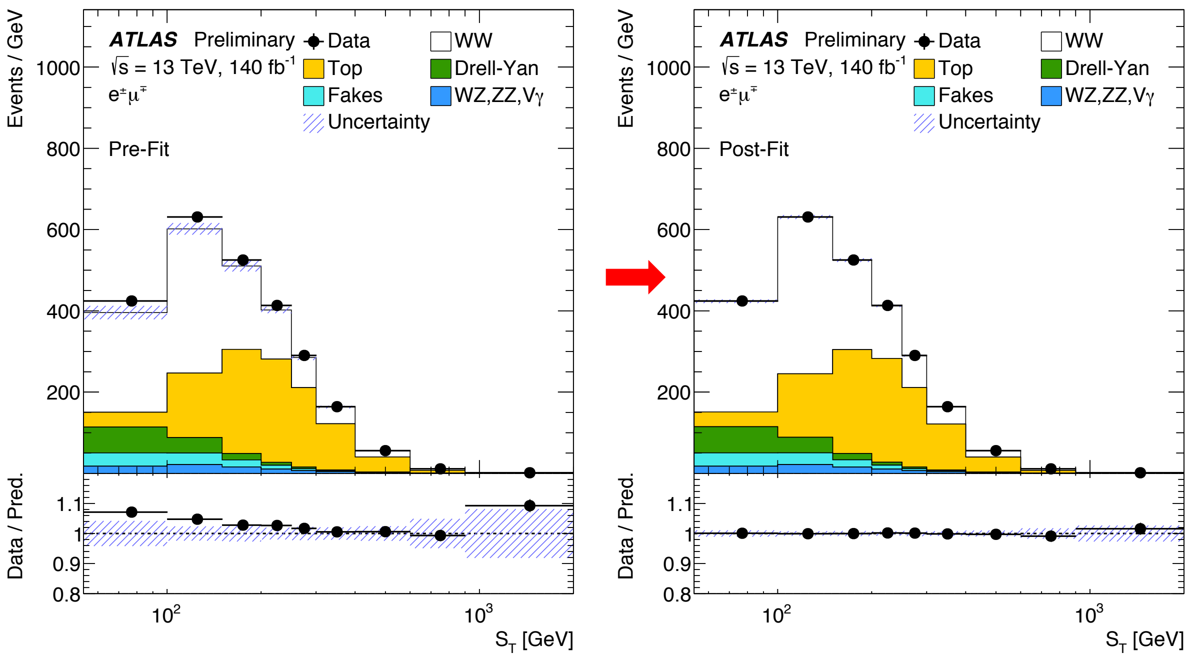

Opposite Sign W^+W^- Cross-Sections

- Fiducial cross section is measured with the 3.1% (!) total uncertainty
  - Excellent agreement with the MATRIX 2.0.1 prediction at nNNLO in QCD NNLO $qq \to WW$ + NLO $gg \to WW$

$$\sigma_{\text{fid}} = 707 \pm 7\ (\text{stat.}) \pm 20\ (\text{syst.})\ \text{fb}$$

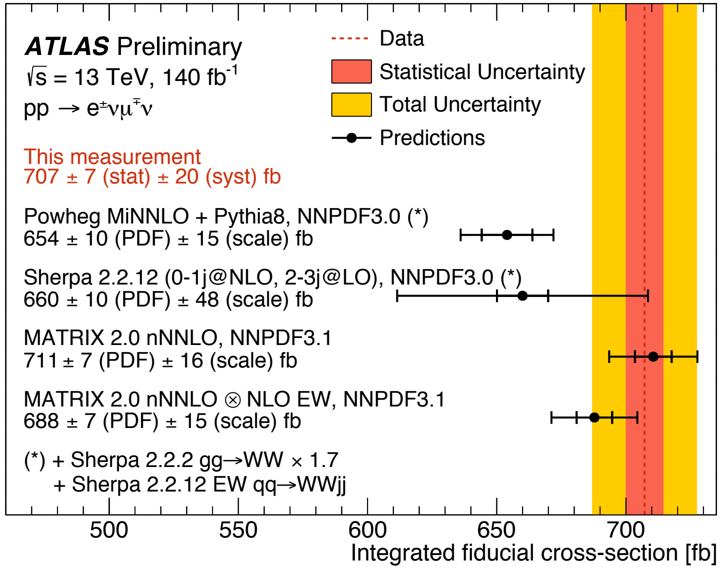

- Total cross section of W^+W^- production is calculated using the acceptance of the $W^+W^- \to e^\pm\nu\mu^\mp\nu$ events: 23.7% $\pm$ 0.3%, and the leptonic W branching ratio: 10.86%

$$\sigma_{\text{total}} = 127 \pm 1\ (\text{stat.}) \pm 4\ (\text{syst.})\ \text{pb}$$

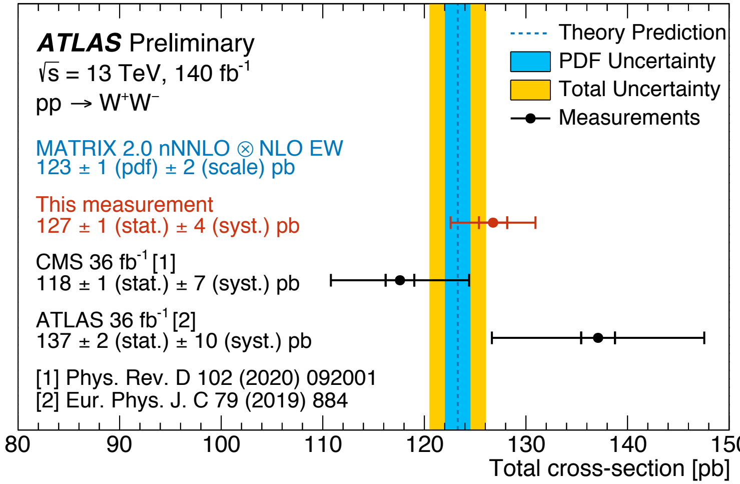

- Differential cross sections are measured for **twelve** observables
  - Iterative Bayesian unfolding used
  - Good agreement with predictions observed

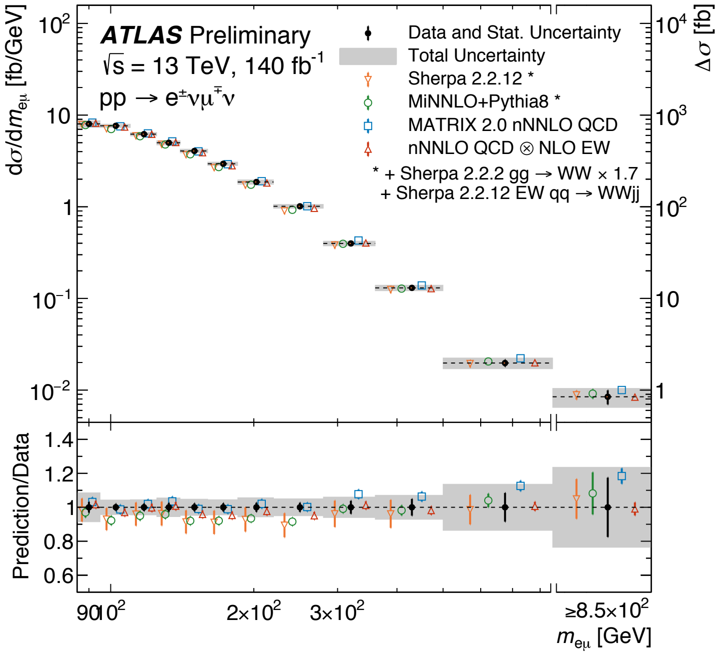

$ZZ(\to 4l)jj$ Differential Cross Sections

JHEP 01 (2024) 004

$\sqrt{s} = 13\,TeV,\ 140\,fb^{-1}$

- Differential cross sections are measured in VBS-enhanced ($\zeta < 0.4$) and VBS-suppressed ($\zeta > 0.4$) regions
  - Three types of observables are measured
    - VBS observables
    - Polarisation, charge conjugation and parity observables
    - QCD-sensitive observables
  - Both EW and QCD production mechanisms are probed
  - Centralities, m_{jj}, $|\Delta y_{jj}|$ and multiplicity of jets (n_{jets}^{gap}) in between the two leading jets are most important observables in EW VBS measurements

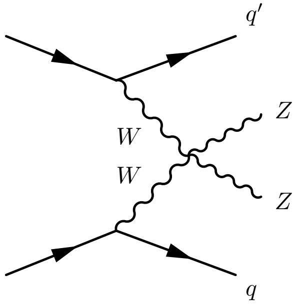

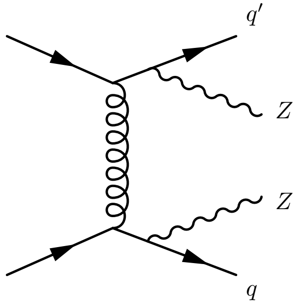

$$\zeta = \left| \frac{\left[y_{4\ell} - 0.5(y_{j_1} + y_{j_2})\right]}{\Delta y_{jj}} \right|$$

- Two Z bosons are selected from the same-flavour opposite-charge lepton pairs
  - Have smallest $|m_{ll} - m_Z|$
  - Are formed from different leptons

Process	Event yield ± stat. ± syst.	
	VBS-enhanced	VBS-suppressed
strong $4\ell jj$ (SHERPA)	$98.9 \pm 0.5 \pm 25.2$	$45.5 \pm 0.3 \pm 12.9$
EW $4\ell jj$ (MG5+PY8)	$24.1 \pm 0.1 \pm 1.8$	$2.12 \pm 0.02 \pm 0.14$
Prompt background	$18.8 \pm 0.2 \pm 2.2$	$5.5 \pm 0.1 \pm 0.4$
Non-prompt background	$3.0 \pm 0.6 \pm 3.2$	$1.1 \pm 0.5 \pm 1.2$
Total prediction	$144 \pm 1 \pm 26$	$54 \pm 1 \pm 13$
Data	169	53

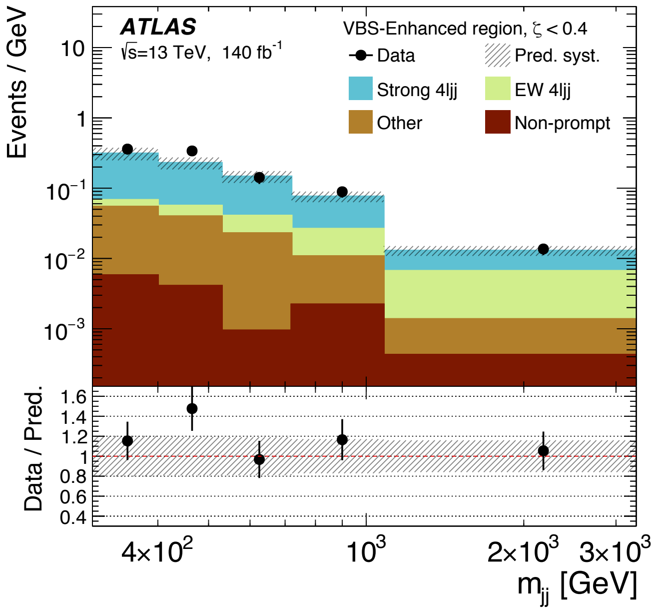

$ZZ(\rightarrow 4l)jj$ Differential Cross Sections

- Iterative Bayesian unfolding is used to measure differential cross sections
- EFT samples combined with the SM signal are fitted to the unfolded m_{4l} and m_{jj} distributions and limits (@ 95% C.L.) on anomalous couplings of dimension-8 operators are obtained

$$\mathcal{L} = \mathcal{L}_{SM} + \sum_i \frac{f_{T,i}}{\Lambda^4} O_{T,i}$$

Much stronger limits are set on these three couplings by the same sign WWjj measurement (presented on the slide #4)

Wilson coefficient	$\lvert \mathcal{M}_{d8} \rvert^2$ Included	95% confidence interval [TeV^{-4}] Expected	95% confidence interval [TeV^{-4}] Observed
$f_{T,0}/\Lambda^4$	yes	[-0.98, 0.93]	[-1.00, 0.97]
	no	[-23, 17]	[-19, 19]
$f_{T,1}/\Lambda^4$	yes	[-1.2, 1.2]	[-1.3, 1.3]
	no	[-160, 120]	[-140, 140]
$f_{T,2}/\Lambda^4$	yes	[-2.5, 2.4]	[-2.6, 2.5]
	no	[-74, 56]	[-63, 62]
$f_{T,5}/\Lambda^4$	yes	[-2.5, 2.4]	[-2.6, 2.5]
	no	[-79, 60]	[-68, 67]
$f_{T,6}/\Lambda^4$	yes	[-3.9, 3.9]	[-4.1, 4.1]
	no	[-64, 48]	[-55, 54]
$f_{T,7}/\Lambda^4$	yes	[-8.5, 8.1]	[-8.8, 8.4]
	no	[-260, 200]	[-220, 220]
$f_{T,8}/\Lambda^4$	yes	[-2.1, 2.1]	[-2.2, 2.2]
	no	[-4.6, 3.1]$\times 10^4$	[-3.9, 3.8]$\times 10^4$
$f_{T,9}/\Lambda^4$	yes	[-4.5, 4.5]	[-4.7, 4.7]
	no	[-7.5, 5.5]$\times 10^4$	[-6.4, 6.3]$\times 10^4$

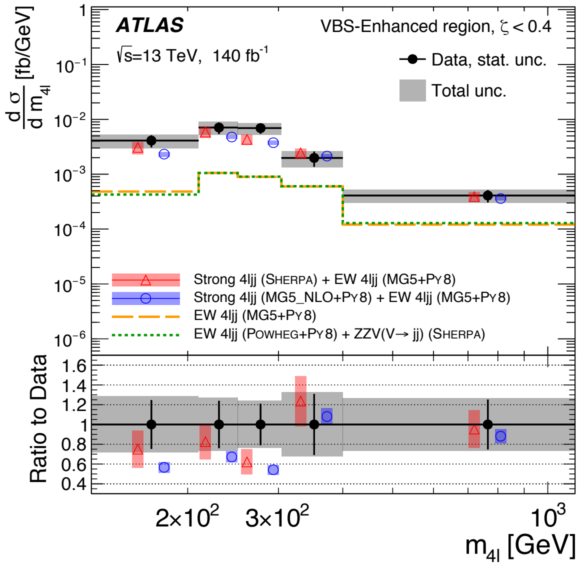

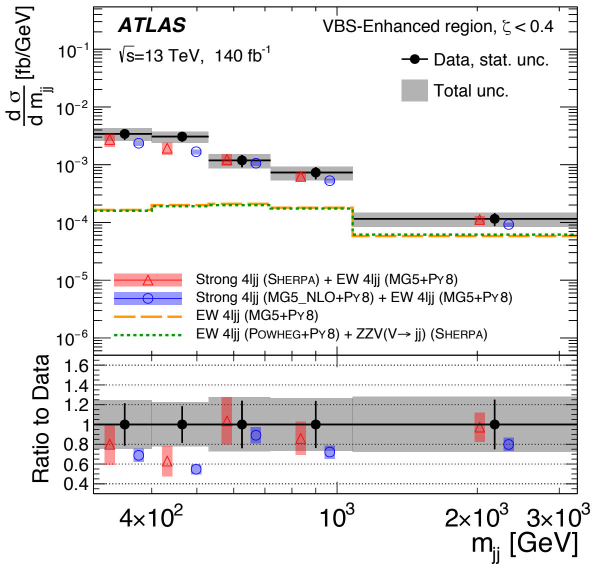

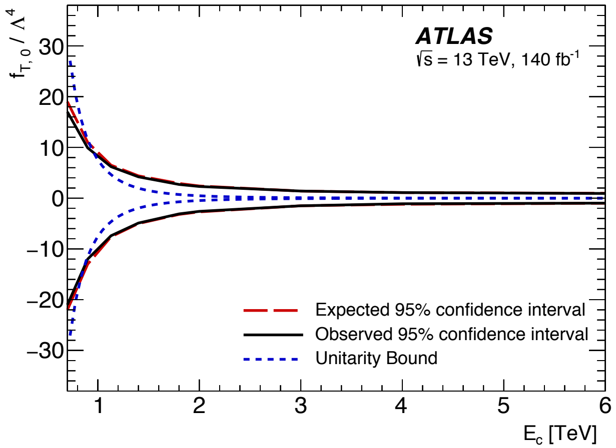

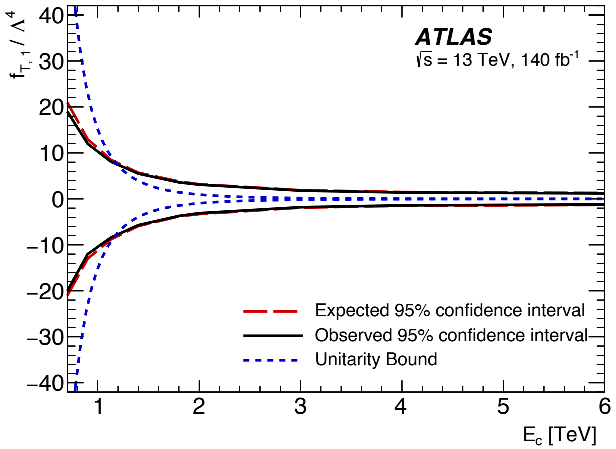

$ZZ \to 4l$ Polarisation and CP Properties

JHEP 12 (2023) 107

$\sqrt{s} = 13\ TeV,\ 140\ fb^{-1}$

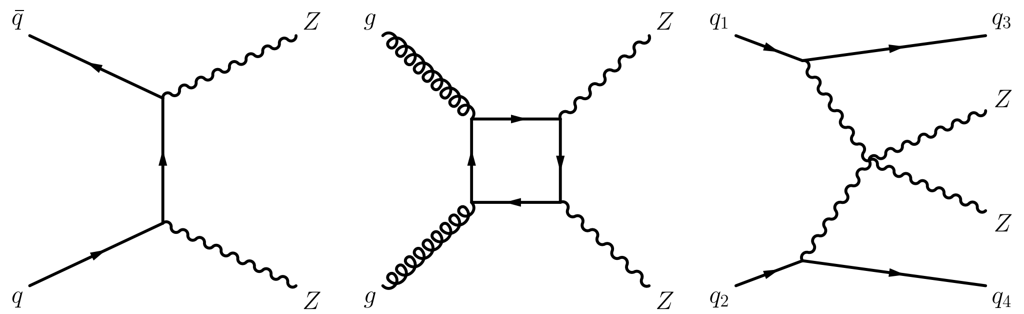

- Production of longitudinally polarised $Z_L Z_L$ bosons is measured in $ZZ \to l^+l^-l'^+l'^-$ final states with $l, l' = e, \mu$
- Profile-likelihood fit to the Boosted Decision Tree classifier is employed to measure the $Z_L Z_L$ and the joined $Z_L Z_T + Z_T Z_T$ polarisation components of the signal
  - The polarisation templates are obtained at the NLO accuracy in both QCD and EW
    - Advanced re-weighting scheme of the LO templates

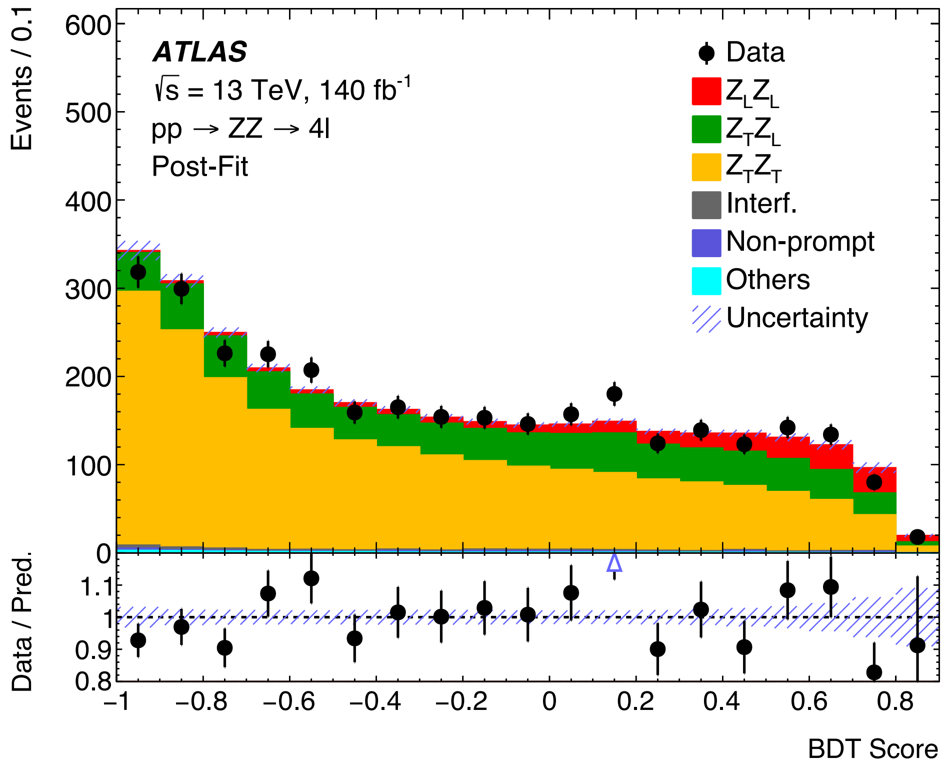

- Observed significance of $Z_L Z_L$ is **4.3σ**
  - **3.8σ** expected
- Fiducial cross section of $Z_L Z_L$ is $\mathbf{2.45 \pm 0.60\ fb}$
  - Consistent with the SM value of $\mathbf{2.10 \pm 0.09\ fb}$
    - Includes QCD and electroweak NLO corrections

$ZZ \rightarrow 4l$ Polarisation and CP Properties

- Differential cross section as a function of **CP-sensitive Optimal Observable** is measured
  - Angular observables: $T_{yz,1(3)} = \sin(\phi_{1(3)}) \times \cos(\theta_{1(3)})$
  - 2D → 1D mapping: $T_{yz,1}{:}T_{yz,3} \rightarrow O_{T_{yz,1}T_{yz,3}}$

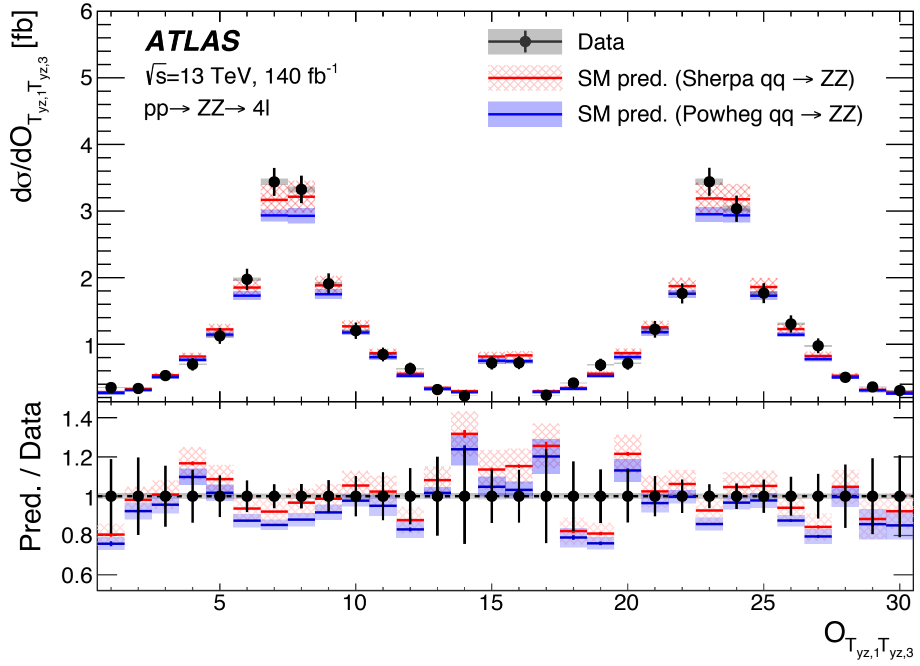

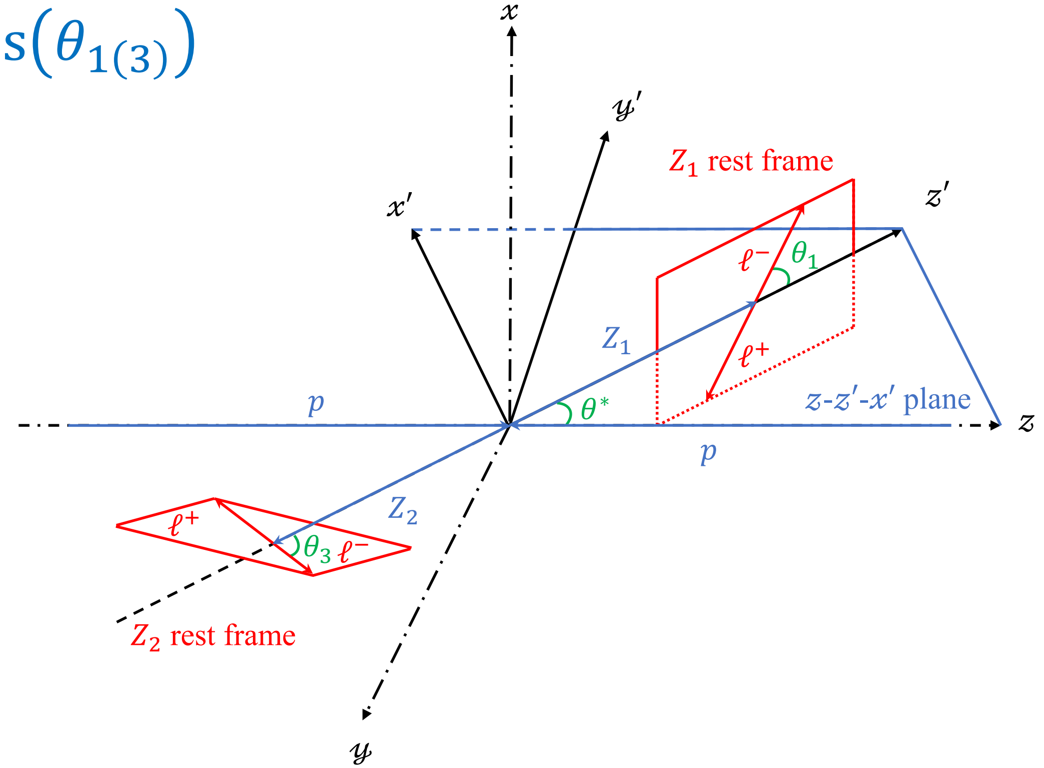

$$\sigma^i = \sigma^i_{\rm SM} + c \cdot \sigma^i_{\rm interference} + c^2 \cdot \sigma^i_{\rm quadratic}$$

- First limits (@ 95% C.L.) on anomalous CP-odd neutral triple gauge couplings, f_Z^4 and f_γ^4, using only the linear interference terms are obtained

aNTGC parameter	Interference only		Full	
	Expected	Observed	Expected	Observed
f_Z^4	[−0.16, 0.16]	[−0.12, 0.20]	[−0.013, 0.012]	[−0.012, 0.012]
f_γ^4	[−0.30, 0.30]	[−0.34, 0.28]	[−0.015, 0.015]	[−0.015, 0.015]

$ZZ \to 4l$ Cross Sections at $\sqrt{s}$ =13.6 TeV

arXiv:2311.09715

$\sqrt{s} = 13.6\,TeV,\ 29\,fb^{-1}$

- ❑ ZZ production is measured first time by the ATLAS in pp-collisions at $\sqrt{s}$ =13.6 TeV
  - ❖ Fiducial and differential cross sections are measured in $4l$ final states
    - ○ Fiducial cross-section is extrapolated to the total cross section satisfying $66 < m_Z < 116$ GeV for both Z

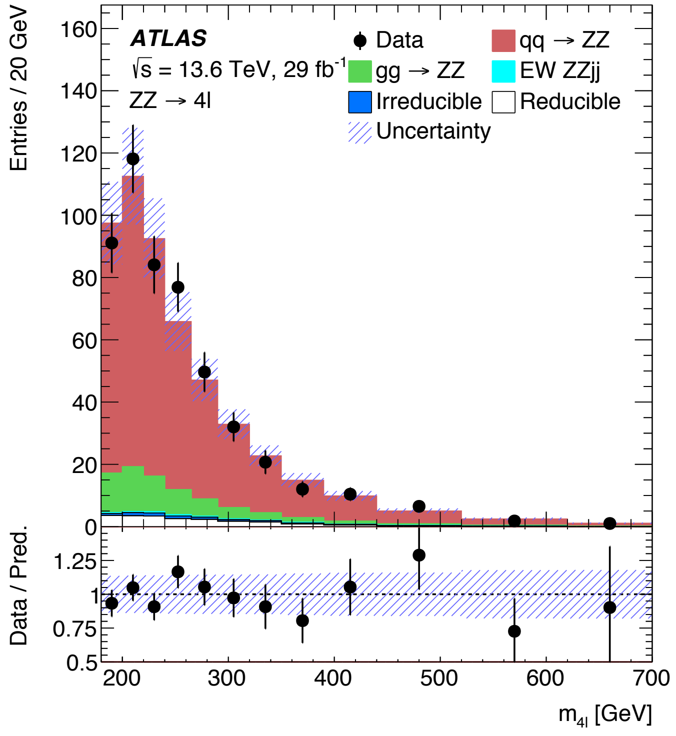

❑ Cut-and-count approach is used

$$\sigma_{fid} = \frac{N_{obs} - N_{bkg}}{\mathcal{L} \times C_{ZZ}}$$

$$C_{ZZ} = 0.555 \pm 0.022$$

$$\sigma_{total} = \frac{\sigma_{fid}}{A_{ZZ} \times BR(ZZ \to 4l)}$$

$$A_{ZZ} = 0.482 \pm 0.003$$

MATRIX calculations @ nNNLO QCD ⊗ NLO EW

❑ Iterative Bayesian unfolding is used

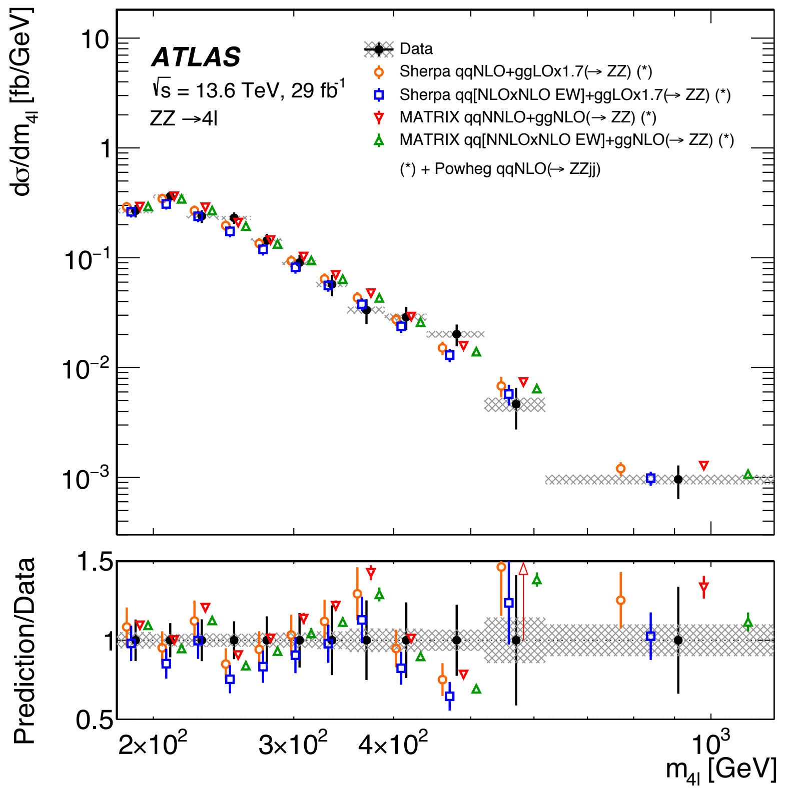

	Measurement	MC prediction	MATRIX prediction
Fiducial	$36.7 \pm 1.6(\text{stat}) \pm 1.5(\text{syst}) \pm 0.8(\text{lumi})$ fb	$36.8\ ^{+4.3}_{-3.5}$ fb	36.5 ± 0.7 fb
Total	$16.8 \pm 0.7(\text{stat}) \pm 0.7(\text{syst}) \pm 0.4(\text{lumi})$ pb	$17.0\ ^{+1.9}_{-1.4}$ pb	16.7 ± 0.5 pb

$Z\gamma jj$ Measurement

Phys. Lett. B 846 (2023) 138222

$\sqrt{s} = 13\ TeV,\ 140\ fb^{-1}$

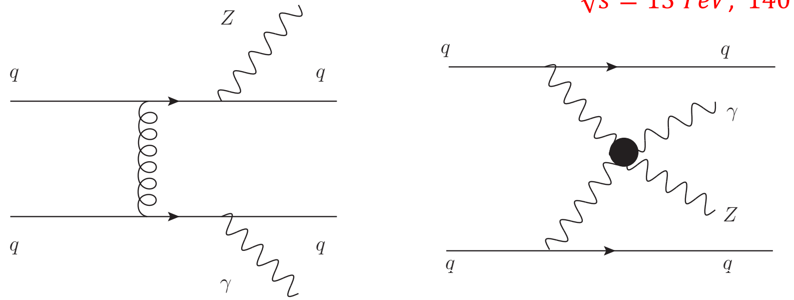

- EW (sensitive to VBS) and extended EW (EW+QCD) production fiducial and differential cross sections are measured in leptonic final states, ee and $\mu\mu$
  - The EW measurements employ a control region to constrain the QCD background
    - SR: $\boldsymbol{\zeta(Z\gamma) < 0.4}$, CR: $\boldsymbol{\zeta(Z\gamma) > 0.4}$

$$\zeta(Z\gamma) = \left|\frac{y_{Z\gamma} - (y_{j_1} + y_{j_2})/2}{y_{j_1} - y_{j_2}}\right|$$

- Profile-likelihood fit to m_{jj} distributions in the SR and CR (in case of the EW measurement) is used to extract signal normalisation → evaluate fiducial cross sections
  - Both EW and extended EW fiducial cross sections are in a good agreement with the SM predictions

EW ($m_{jj} > 500\ GeV$): $\sigma_{\text{EW}} = 3.6 \pm 0.5$ fb, $\sigma_{\text{EW}}^{pred} = 3.5 \pm 0.2$ fb

Extended EW ($m_{jj} > 150\ GeV$): $\sigma_{Z\gamma} = 16.8^{+2.0}_{-1.8}$ fb, $\sigma_{Z\gamma}^{pred} = 15.7^{+5.0}_{-2.6}$ fb

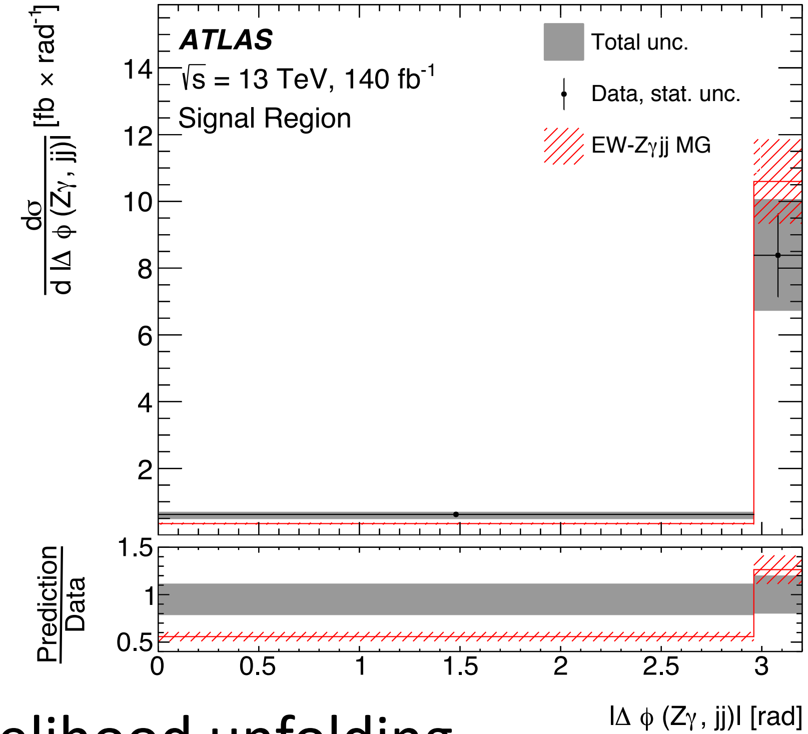

- Differential cross sections are measured using profile-likelihood unfolding
  - Unfolded observables are in a good agreement with SM distributions except of $|\Delta\boldsymbol{\phi}(\boldsymbol{Z\gamma, jj})|$
    - About two standard deviation is observed in the lowest bin of the EW measurement

Observation of $W\gamma\gamma$

[Phys. Lett. B 848 (2024) 138400]

$\sqrt{s} = 13\ TeV,\ 140\ fb^{-1}$

- $W\gamma\gamma$ production in e/μ final states is observed first time with significance of **5.6σ** (observed and expected)
  - Main background is due to the jet-to-photon and electron-to-photon misidentification

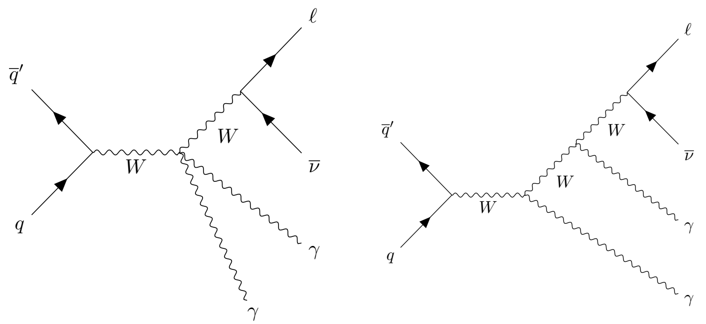

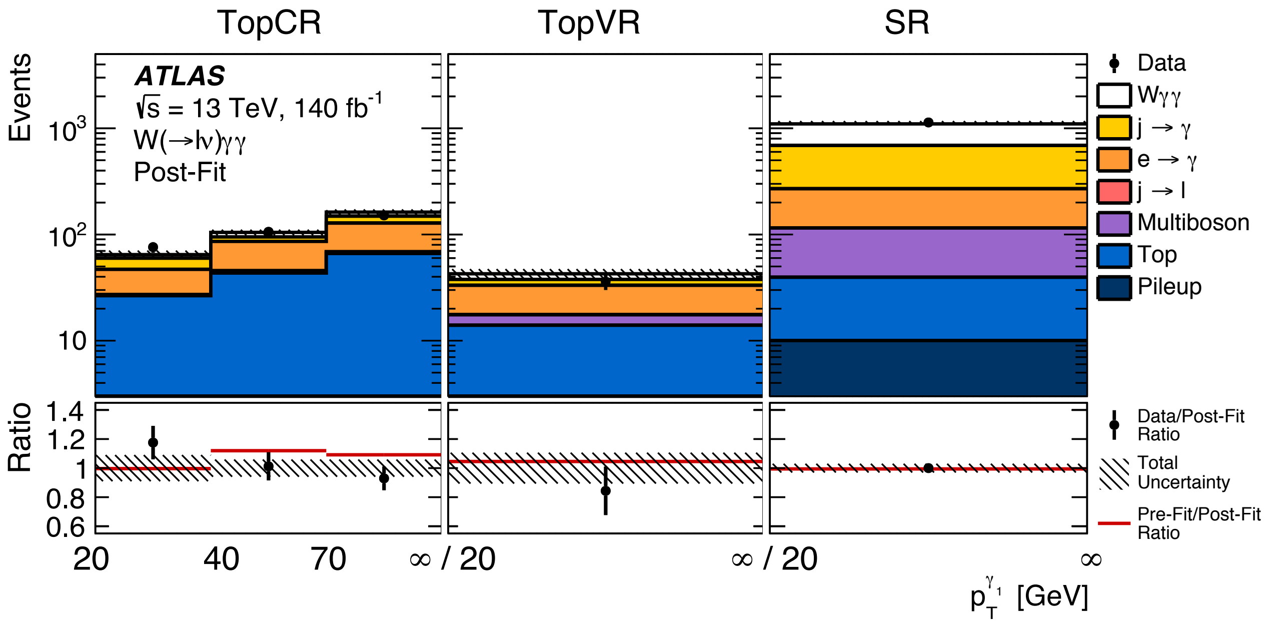

$$\sigma_{fid}^{e/\mu} = \frac{N_{signal}}{\mathcal{L} \times C}$$

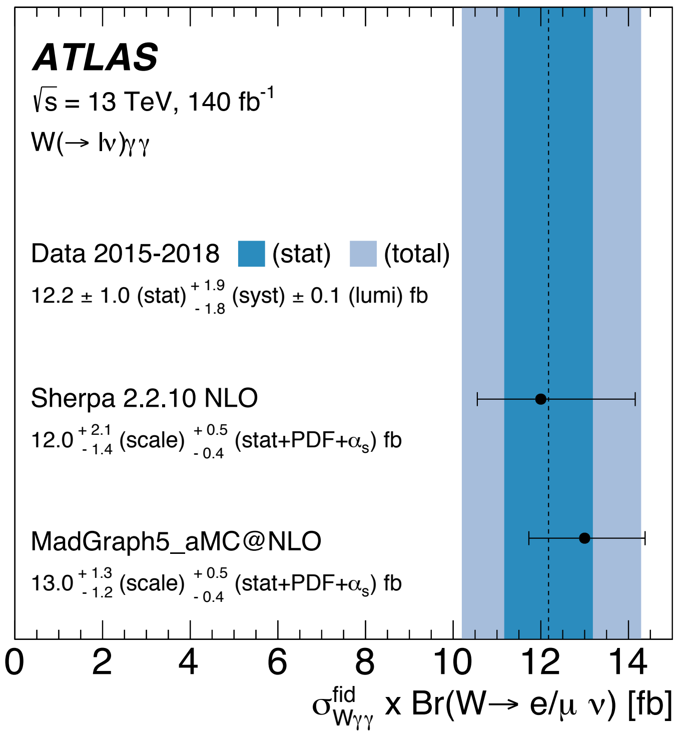

- Fiducial cross section is measured for combined $W \to e\nu/\mu\nu$ events with total 17% uncertainty
  - Leptonically decaying τ-leptons are not considered

Observation of $WZ\gamma$

Phys. Rev. Lett. 132 (2024) 021802

$\sqrt{s} = 13\ TeV,\ 140\ fb^{-1}$

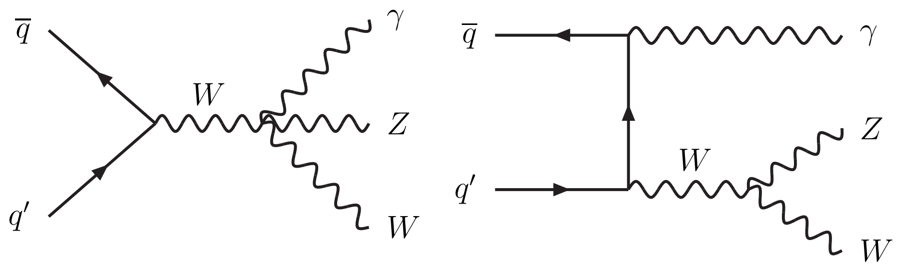

- ❑ $WZ\gamma \to l'^{\pm}\nu l^{+}l^{-}\nu\gamma$ production, where $l^{(\prime)} = e, \mu$, is observed first time with significance of **6.3σ** (expected **5.0σ**)
  - ❖ Dominant background stems from the non-prompt leptons and photons from hadronic decays and from misidentified jets
- ❑ Profile-likelihood fit is done to the signal and two control regions for $ZZ\gamma$ and $ZZ(e \to \gamma)$ backgrounds
  - ❖ Three normalization parameters for the signal and the two backgrounds are fitted simultaneously
  - ❖ All leptonic final state events $(eee, \mu\mu\mu, ee\mu, e\mu\mu)$ are combined in the fit
- ❑ Fitted signal normalization parameter $\mu_{WZ\gamma}$ is used to measure the fiducial cross section
  - ❖ $\sigma^{obs}_{fid} = 2.0 \pm 0.30\ (stat.) \pm 0.16\ (syst.)\ fb$
    - ○ Consistent with the $\sigma^{SM}_{fid} = 1.50 \pm 0.06\ (tot.)\ fb$ within 1.5σ

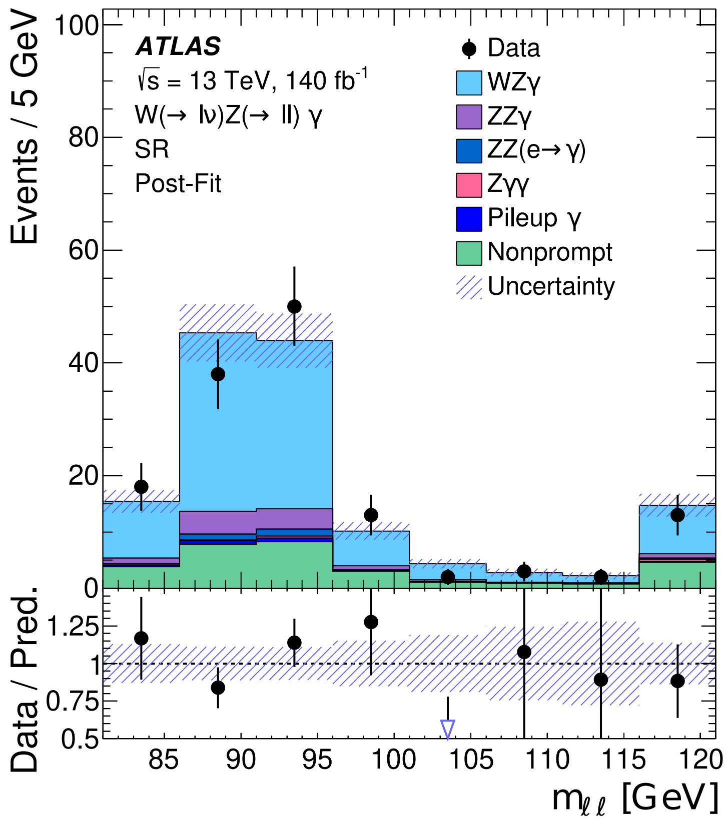

Summary

- ❑ Measurements of multiboson production processes allow to test the gauge interactions of the SM electroweak theory and its symmetry breaking mechanism

- ❑ Multiboson production final states have relatively small cross sections even at the LHC energy and can be very sensitive to new physics effects leading to anomalous triple and quartic gauge couplings

- ❑ First time observations and precise measurements of various multiboson production processes became possible in proton-proton collision data collected by the LHC experiments, CMS and ATLAS

- ❑ Latest results of the experimental studies of multiboson interactions in the ATLAS detector were discussed
    - ❖ All presented results are consistent with the Standard Model predictions within the measurement uncertainties

Thank you!

Electroweak Vector Boson Scattering

- Electroweak VBS processes $V_1 V_2 \rightarrow V_3 V_4$ have not been studied experimentally before the LHC experiments
  - Low production cross sections even at the LHC energies
    - Sensitivity to possible new physics effects leading to anomalous quartic gauge couplings

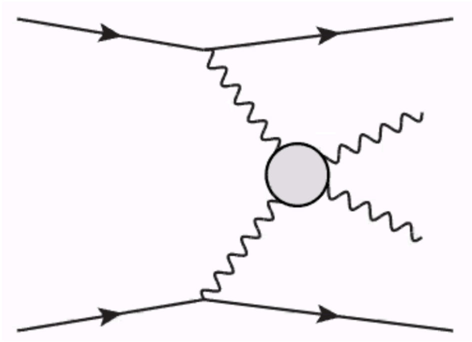

- VBS can involve all or some of the leading order diagrams shown below
  - Depending on the involved vector bosons

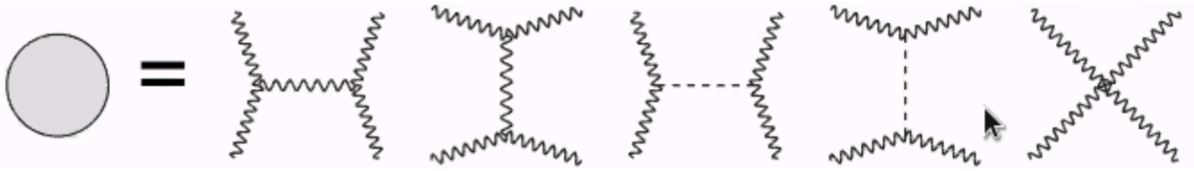

Electroweak Vector Boson Scattering

- Diagrams with Higgs boson are crucial to avoid a unitarity violation due to the rising scattering cross section of the longitudinally polarized W bosons: $\boldsymbol{W_L W_L \rightarrow W_L W_L}$

A. Denner & T. Hahn, Nucl.Phys.B525:27–50,1998

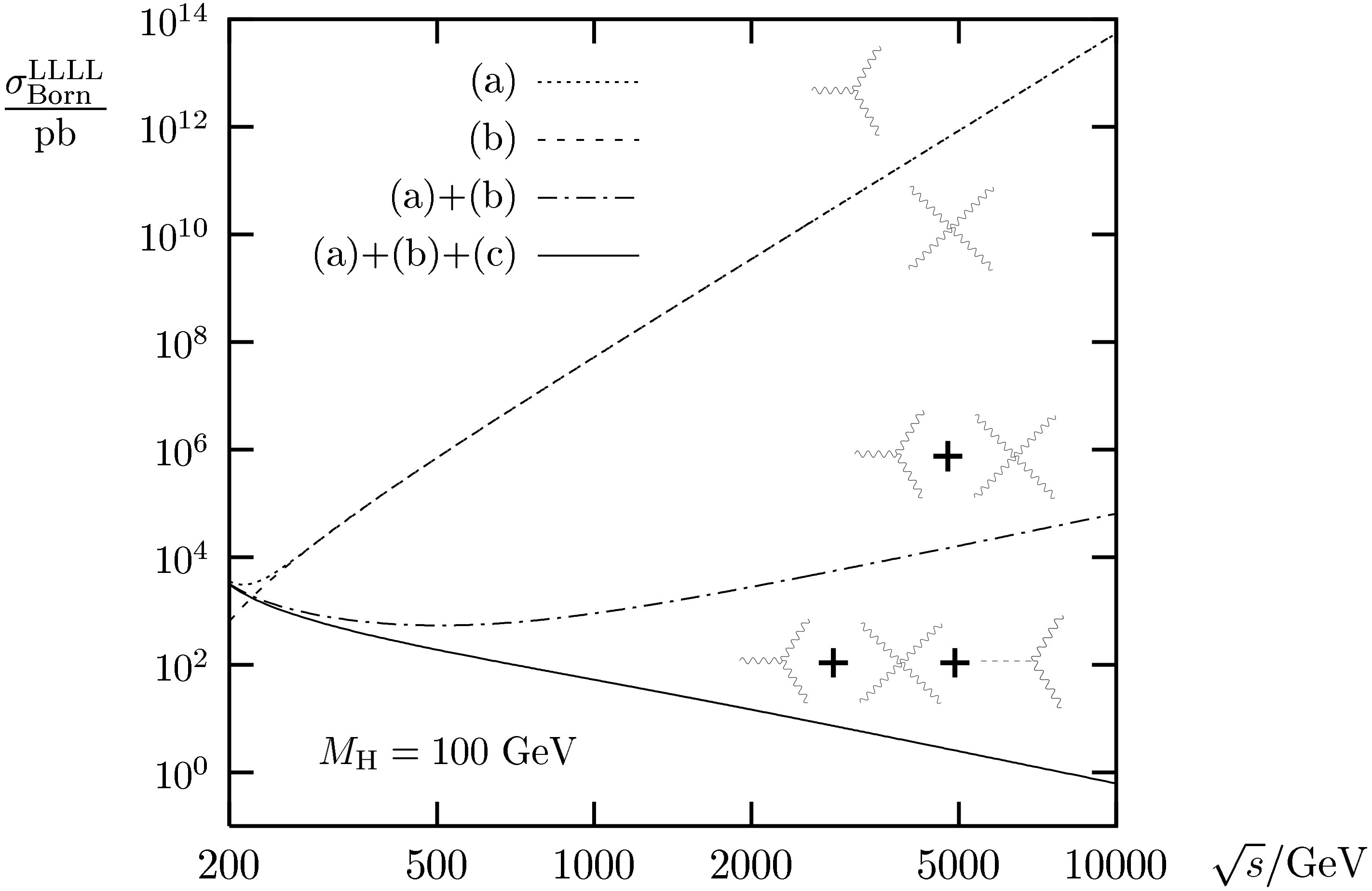

New Physics Searches – Anomalous Gauge Couplings

- Low energy effective field theory (EFT) to parameterize indirect new physics effects with the help of high dimension (n>4) operators $\mathcal{O}_i^{(n)}$ → aTGC and aQGC
  - Linear realization of the SM $SU(2)_L \otimes U(1)_Y$ gauge symmetry

$$\mathcal{L}_{\text{eff}} = \mathcal{L}_{\text{SM}} + \sum_{n=5}^{\infty} \sum_{i} \frac{f_i^{(n)}}{\Lambda^{n-4}} \mathcal{O}_i^{(n)}$$

Eboli et al., 2020

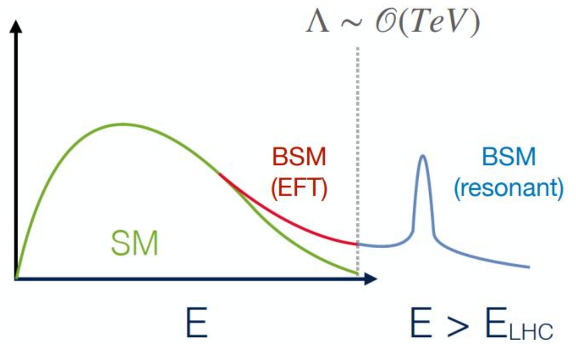

- Lowest order operators that generate aQGC (but not aTGC) are dimension-8 operators

	WWWW	WWZZ	ZZZZ	WWAZ	WWAA	ZZZA	ZZAA	ZAAA	AAAA
$\mathcal{O}_{S,0}$, $\mathcal{O}_{S,1}$	X	X	X						
$\mathcal{O}_{M,0}$, $\mathcal{O}_{M,1}$, $\mathcal{O}_{M,6}$, $\mathcal{O}_{M,7}$	X	X	X	X	X	X	X		
$\mathcal{O}_{M,2}$, $\mathcal{O}_{M,3}$, $\mathcal{O}_{M,4}$, $\mathcal{O}_{M,5}$		X	X	X	X	X	X		
$\mathcal{O}_{T,0}$, $\mathcal{O}_{T,1}$, $\mathcal{O}_{T,2}$	X	X	X	X	X	X	X	X	X
$\mathcal{O}_{T,5}$, $\mathcal{O}_{T,6}$, $\mathcal{O}_{T,7}$		X	X	X	X	X	X	X	X
$\mathcal{O}_{T,8}$, $\mathcal{O}_{T,9}$			X			X	X	X	X

TABLE II: Quartic vertices modified by each dimension-8 operator are marked with X.

Degrande et al., 2013

- Precise measurements of VBS processes allow to measure the corresponding Wilson coefficients $f_i^{(8)}$ (look for significant deviations from zero, or set limits)

EFT Samples in EW Measurements

$$\mathcal{L}_{\text{eff}} = \mathcal{L}_{\text{SM}} + \sum_i \frac{f_i^{(6)}}{\Lambda^2} O_i + \sum_j \frac{f_j^{(8)}}{\Lambda^4} O_j + \ldots$$

- EFT “model” for the new physics: only dimension-8 operators have non-zero coefficients
  - ✦ New physics affects only the quartic gauge couplings
- Amplitude of a VBS process with EFT contributions: $|A_{\text{SM}} + \sum_i c_i A_i|$ $\quad c_i = \frac{f_i^{(8)}}{\Lambda^4}$
- Standard Model, interference, quadratic and cross terms of the total squared amplitude:

$$|A_{\text{SM}} + \sum_i c_i A_i|^2 = |A_{\text{SM}}|^2 + \sum_i c_i 2Re(A_{\text{SM}}^* A_i) + \sum_i {c_i}^2 |A_i|^2 + \sum_{ij, i \neq j} c_i c_j 2Re(A_i A_j^*)$$

- MC samples are generated using only individual terms at a time
- Only one c_i or one pair of c_i and c_j (for generation of cross term samples) are set to nonzero values at a time
  - ✦ Respective sample can be scaled by appropriate c_i, c_i^2, or $c_i c_j$

Same Sign $W^{\pm}W^{\pm}jj$ Measurement

❑ Monte-Carlo signal and background samples

Process, short description	ME Generator + parton shower	Order	Tune	PDF set in ME
EW, Int, QCD $W^{\pm}W^{\pm}jj$, nominal signal	MadGraph5_aMC@NLO2.6.7 + Herwig7.2	LO	Herwig	NNPDF3.0nlo
EW, Int, QCD $W^{\pm}W^{\pm}jj$, alternative shower	MadGraph5_aMC@NLO2.6.7 + Pythia8.244	LO	A14	NNPDF3.0nlo
EW $W^{\pm}W^{\pm}jj$, NLO pQCD approx.	Sherpa2.2.11 & Sherpa2.2.2(WWW) & Powheg Box2+Pythia8.235 (WH)	+0,1j@LO NLO	Sherpa A14	NNPDF3.0nnlo
EW $W^{\pm}W^{\pm}jj$, NLO pQCD approx.	Powheg Boxv2 + Pythia8.230	NLO (VBS approx.)	AZNLO	NNPDF3.0nlo
QCD $W^{\pm}W^{\pm}jj$, NLO pQCD approx.	Sherpa2.2.2	+0,1j@LO	Sherpa	NNPDF3.0nnlo
QCD $VVjj$	Sherpa2.2.2	+0,1j@NLO; +2,3j@LO	Sherpa	NNPDF3.0nnlo
EW $W^{\pm}Z/\gamma^{*}jj$	MadGraph5_aMC@NLO2.6.2+Pythia8.235	LO	A14	NNPDF3.0nlo
EW $Z/\gamma^{*}Z/\gamma^{*}jj$	Sherpa2.2.2	LO	Sherpa	NNPDF3.0nnlo
QCD $V\gamma jj$	Sherpa2.2.11	+0,1j@NLO; +2,3j@LO	A14	NNPDF3.0nnlo
EW $V\gamma jj$	MadGraph5_aMC@NLO2.6.5+Pythia8.240	LO	A14	NNPDF3.0nlo
VVV	Sherpa2.2.1 (leptonic) & Sherpa2.2.2 (one $V \to jj$)	+0,1j@LO	Sherpa	NNPDF3.0nnlo
$t\bar{t}V$	MadGraph5_aMC@NLO2.3.3.p0 + Pythia8.210	NLO	A14	NNPDF3.0nlo
tZq	MadGraph5_aMC@NLO2.3.3.p1 + Pythia8.212	LO	A14	NNPDF2.3lo
$W^{\pm}W^{\pm}jj$ EFT	MadGraph5_aMC@NLO 2.6.5 + Pythia8.235	LO	A14	NNPDF3.0nlo
$H_5^{\pm\pm}$	MadGraph5_aMC@NLO 2.9.5 + Pythia8.245	LO	A14	NNPDF3.0nlo

Same Sign $W^{\pm}W^{\pm}jj$ Measurement

- Event selection signal and control regions
  - CRs for constraining $WZjj$, non-prompt and charge miss-identified lepton backgrounds

Requirement	SR	Low-m_{jj} CR	WZ CR
Leading and subleading lepton p_T	> 27 GeV		
Electron $\|\eta\|$	< 2.47 (1.37 in ee), excluding $1.37 \leq \|\eta\| \leq 1.52$		
Muon $\|\eta\|$	< 2.5		
Leading (subleading) jet p_T	$> 65\,(35)$ GeV		
Additional jet p_T	> 25 GeV		
Jet $\|\eta\|$	< 4.5		
$m_{\ell\ell}$	> 20 GeV		
E_T^{miss}	> 30 GeV		
Charge misid. $Z \to ee$ veto	$\|m_{ee} - m_Z\| > 15$ GeV		–
b-jet veto	$N_{b\text{-jet}} = 0$, $p_T^{b\text{-jet}} > 20$ GeV, $\|\eta^{b\text{-jet}}\| < 2.5$		
$N_{\text{veto leptons}}$	$= 0$	$= 0$	$= 1$, $p_T > 15$ GeV
$m_{\ell\ell\ell}$	–	–	> 106 GeV
m_{jj}	> 500 GeV	$200 < m_{jj} < 500$ GeV	> 200 GeV
$\|\Delta y_{jj}\|$	> 2		

- Data, signal and background pre-fit event yields in the SR
  - Sub-regions defined by the same sign lepton flavours
    - 2 sub-regions for electron-muon pairs by distinguished by the leading pT lepton flavour

Process	ee	$e\mu$	μe	$\mu\mu$	Combined
$W^{\pm}W^{\pm}jj$ EW	27.6 ± 0.9	68.2 ± 1.6	61.3 ± 1.5	77.8 ± 1.7	235 ± 5
$W^{\pm}W^{\pm}jj$ QCD	1.6 ± 0.5	7.3 ± 2.2	6.4 ± 1.9	8.8 ± 2.5	24 ± 7
$W^{\pm}W^{\pm}jj$ Int	0.93 ± 0.20	2.2 ± 0.5	2.0 ± 0.4	2.5 ± 0.5	7.6 ± 1.6
$W^{\pm}Zjj$ QCD	8.4 ± 1.0	26.8 ± 3.0	26.7 ± 3.0	20.9 ± 2.2	83 ± 9
$W^{\pm}Zjj$ EW	1.71 ± 0.14	4.9 ± 0.4	4.1 ± 0.4	4.2 ± 0.4	14.9 ± 1.2
Non-prompt	8.9 ± 2.6	15 ± 4	10.2 ± 3.2	21 ± 7	56 ± 12
$V\gamma$	1.3 ± 0.8	5.1 ± 2.2	4.6 ± 2.6	—	11 ± 5
Charge misid.	3.8 ± 2.0	5.0 ± 1.3	1.2 ± 0.4	—	10 ± 4
Other prompt	1.02 ± 0.29	2.5 ± 0.6	1.8 ± 0.5	1.7 ± 2.2	7.1 ± 2.8
Total expected	55 ± 4	137 ± 7	118 ± 6	137 ± 8	448 ± 20
Data	52	149	127	147	475

Same Sign $W^{\pm}W^{\pm}jj$ Measurement

- Unfolding results obtained with maximum likelihood fit method

$$m_{\mathrm{T}} = \sqrt{\left(E_{\mathrm{T}}^{\ell\ell} + E_{\mathrm{T}}^{\mathrm{miss}}\right)^2 - \left|\vec{p}_{\mathrm{T}}^{\,\ell\ell} + \vec{E}_{\mathrm{T}}^{\mathrm{miss}}\right|^2}$$

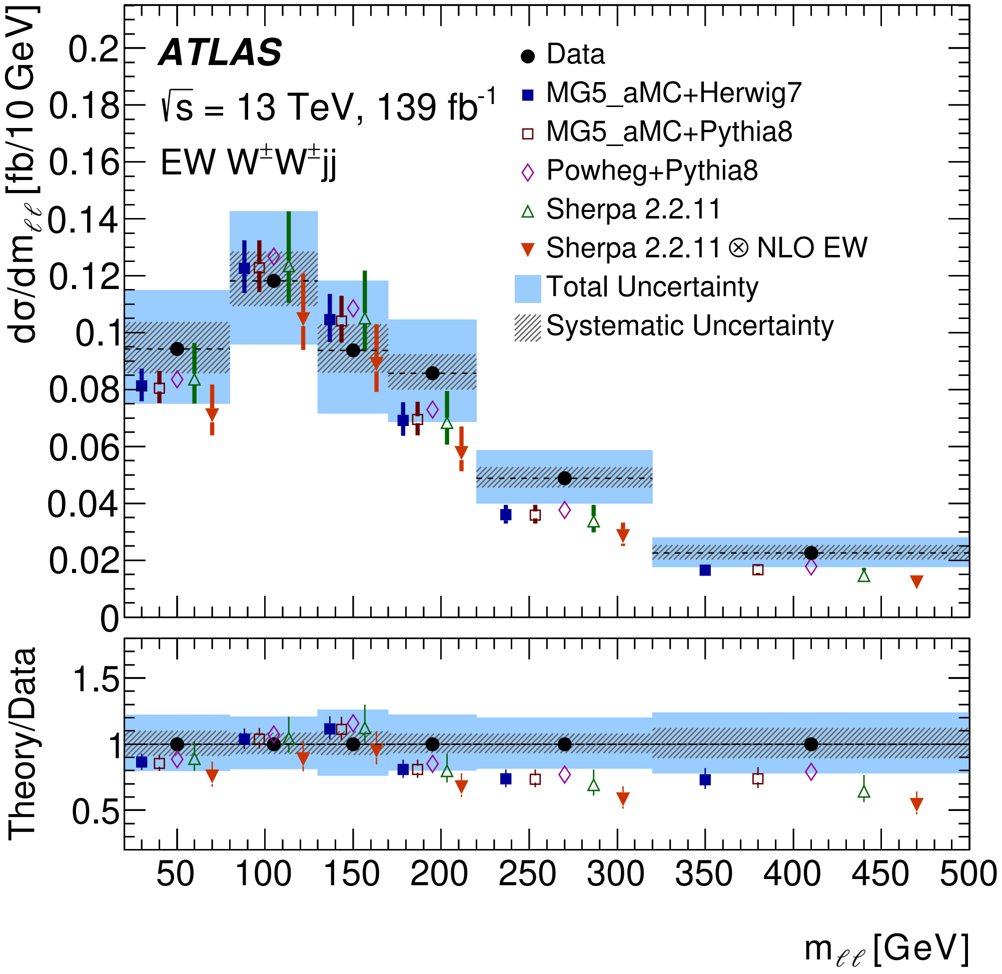

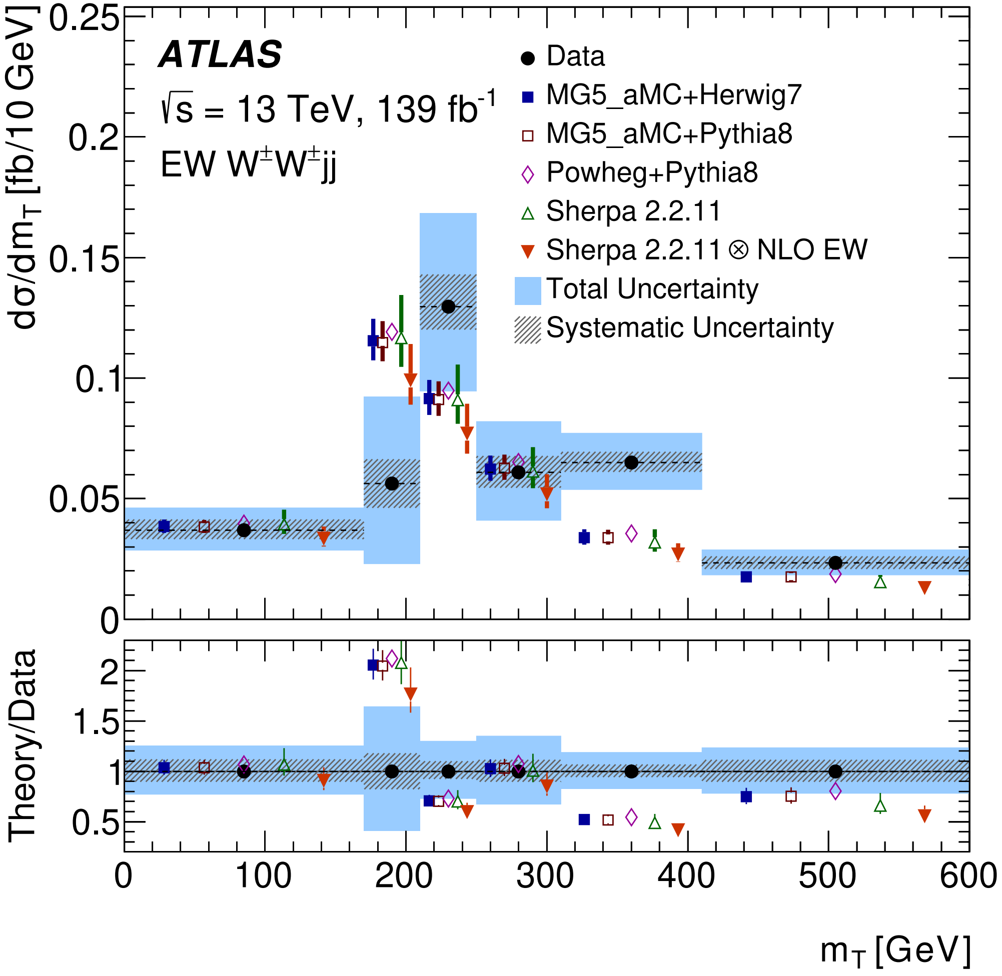

Same Sign $W^{\pm}W^{\pm}jj$ Measurement

❑ Unfolding results obtained with maximum likelihood fit method

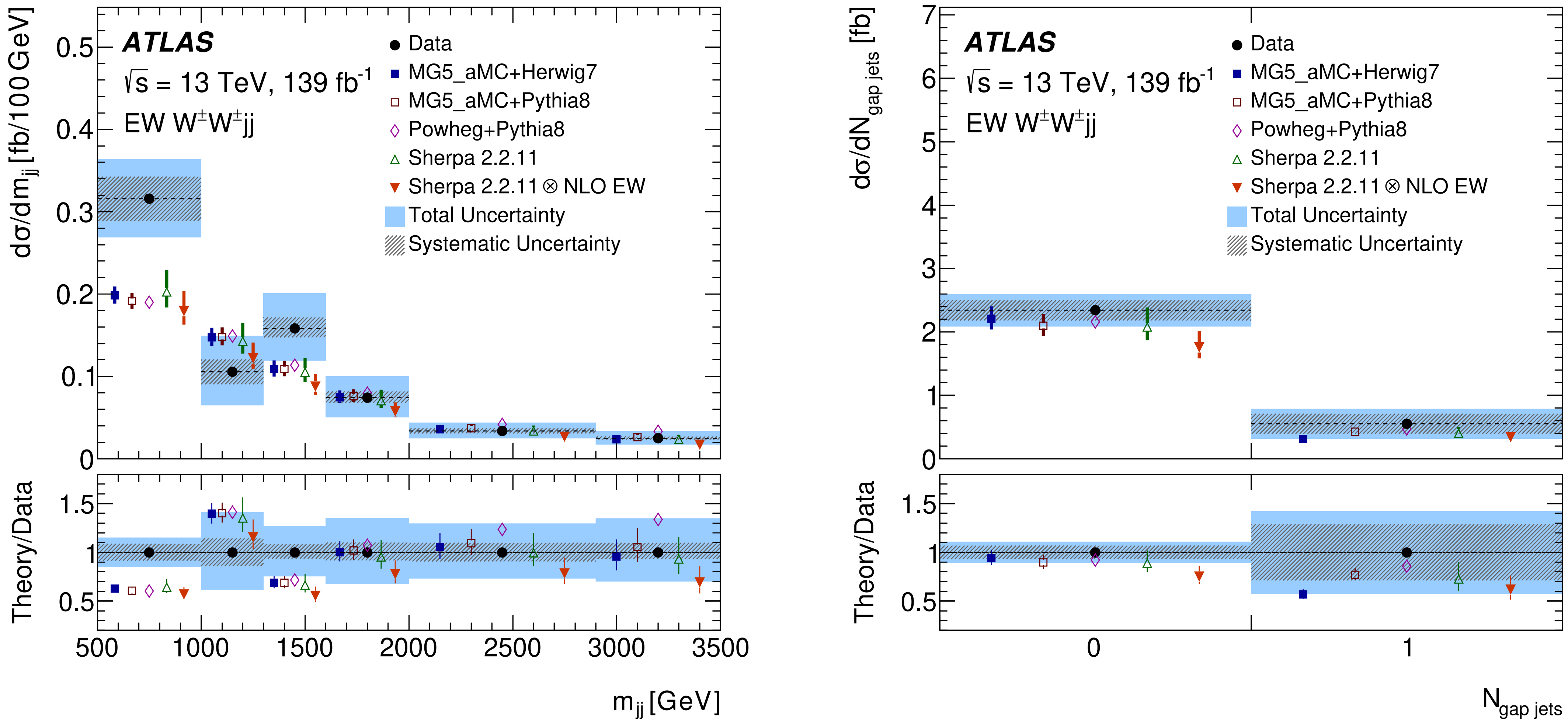

Same Sign $W^{\pm}W^{\pm}jj$ Measurement

- ❑ Search for the doubly charged Higgs boson of the GM (Georgi and Machacek) model
- ❑ Excess observed at the $m_T = 450$ GeV with a local (global) significance of 3.3σ (2.5σ)

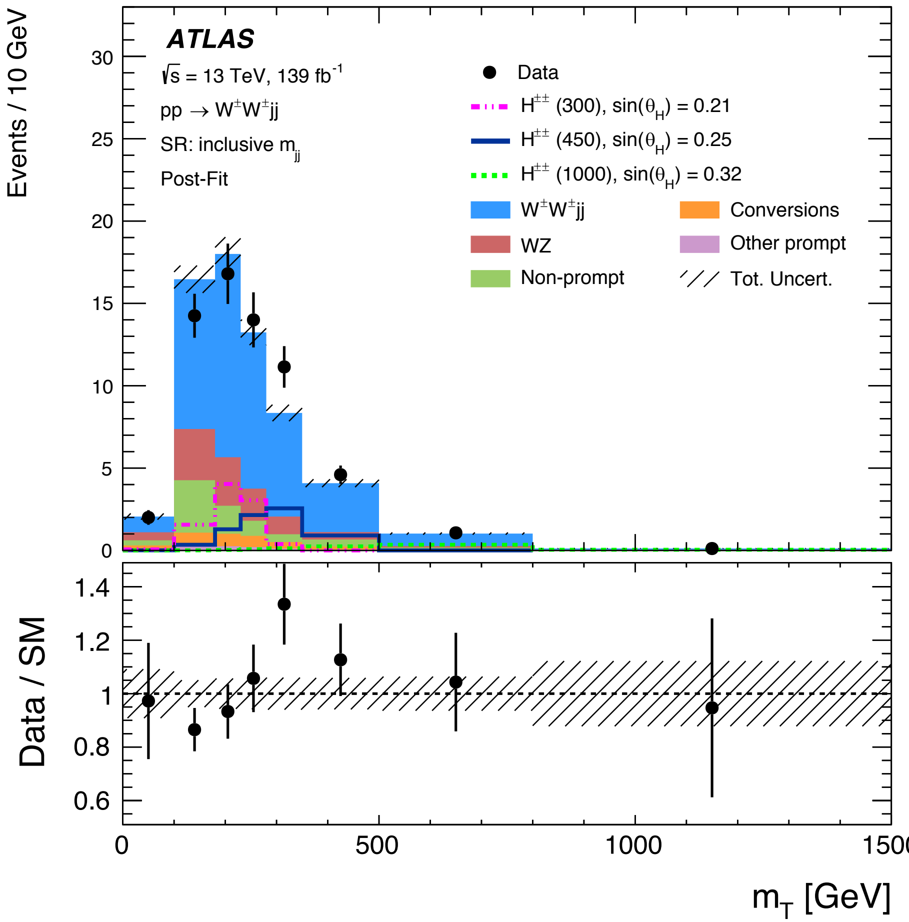

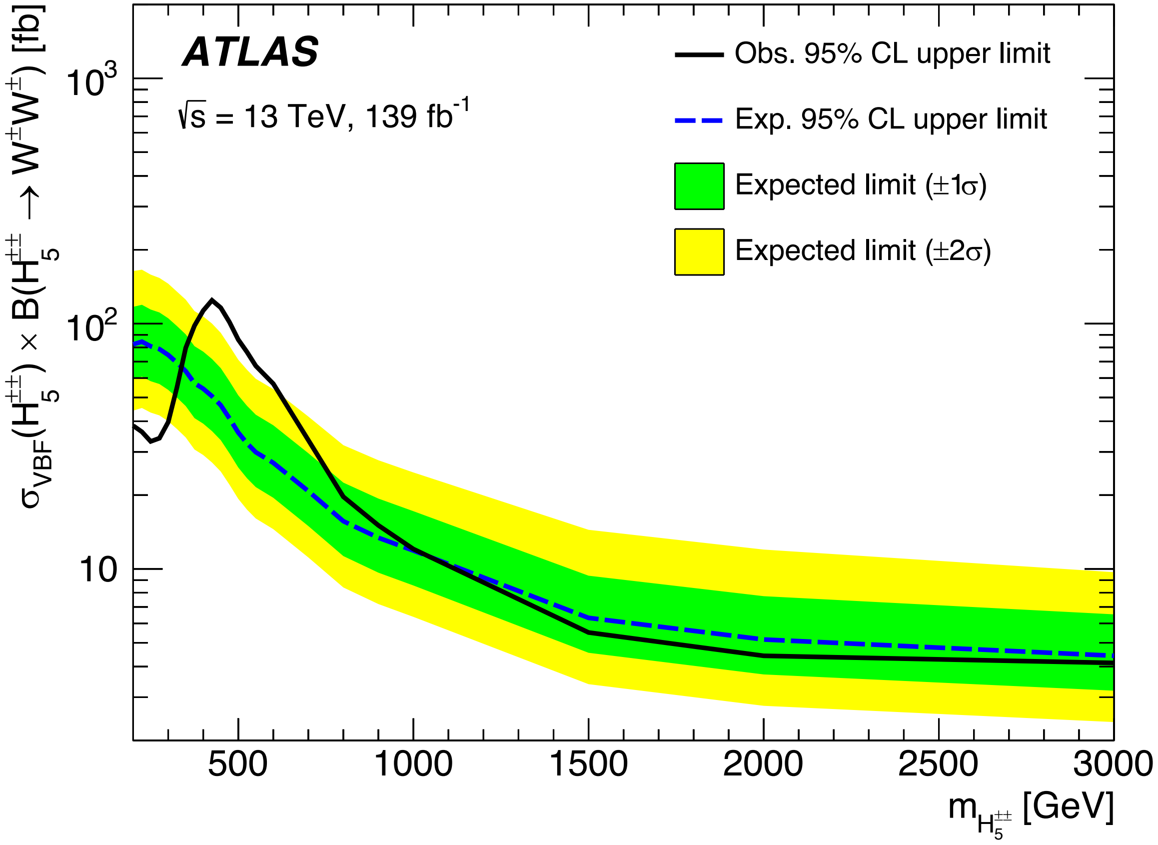

$ZZ \to 4l$ Polarisation and CP Properties

- $qq \to ZZ$ polarisation samples for three helicity states $Z_L Z_L$, $Z_L Z_T$ and $Z_T Z_T$ are generated with MadGraph5 at the LO accuracy in QCD

- $gg \to ZZ$ polarisation samples are obtained with dedicated MC event reweighting method from the inclusive Sherpa sample

- Polarisation and their interference samples are corrected to the NLO accuracy in both QCD and EW

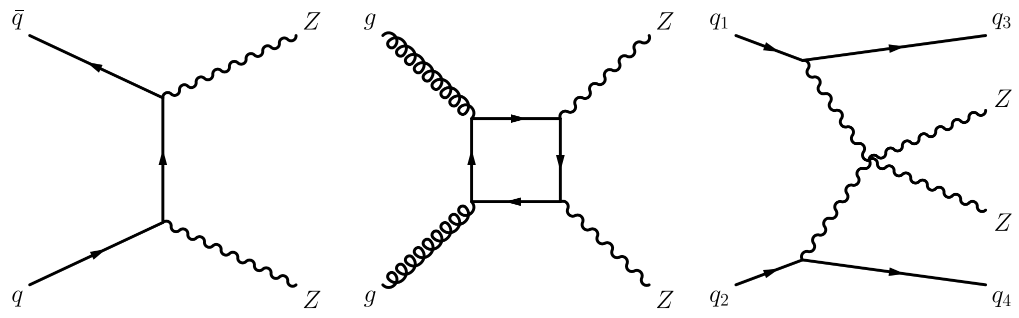

- Boosted Decision Tree classifier is used to discriminate signal from background

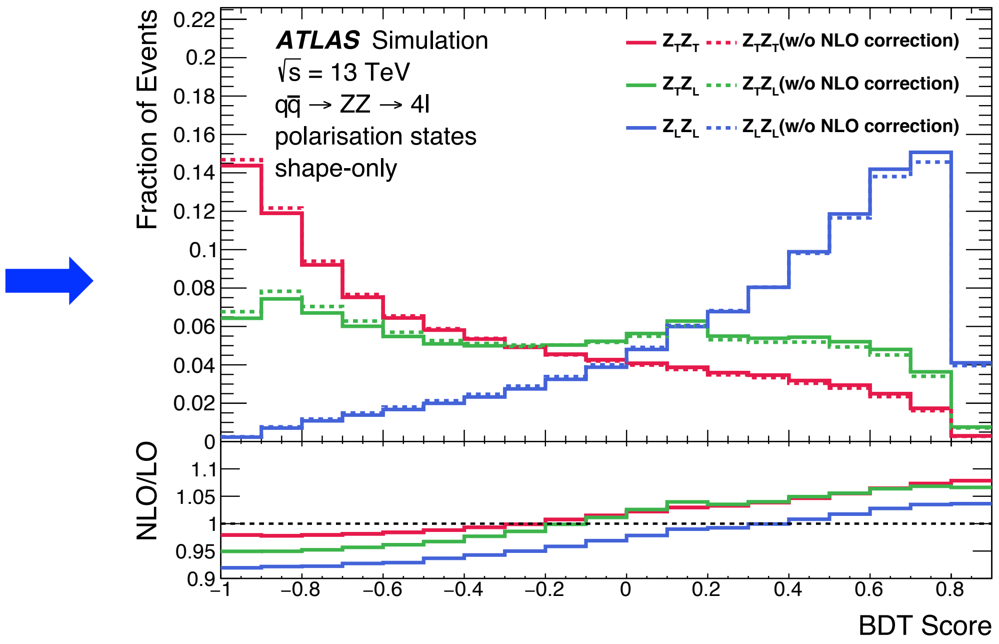

$ZZ \rightarrow 4l$ Polarisation and CP Properties

- Supporting material

		Pre-fit	Post-fit
ZZ	$Z_L Z_L$	189.3 ± 8.7	220 ± 54
	$Z_T Z_L$	710 ± 29	711 ± 29
	$Z_T Z_T$	2170 ± 120	2147 ± 60
	Interference	33.7 ± 2.8	33.4 ± 2.7
Non-prompt		18.7 ± 7.1	18.5 ± 7.0
Others		20.0 ± 3.7	19.9 ± 3.7
Total		3140 ± 150	3149 ± 57
Data		3149	3149